concentrations, the photoreaction does not appear to occur, presumably because the back-reaction proceeds faster than the photolysis. Likewise, at sufficiently low concentrations the back-reaction of the photolyzed complex is not observed. Titration of the resultant yellow solution (at concentrations where the back-reaction is negligible) with ferrous sulfate yielded Prussian blue, which was then filtered out of the solution. The remaining filtrate showed a UV-vis absorption at the same wavelength as that of $Pt(NH_3)_4(NO_3)_2$. These results demonstrate that the starting products are regenerated upon photolysis by irradiation into the IT band. Others have reported charge-transfer photoreactions for binuclear cyanide-bridged species.[4] Vogler, for example, demonstrated that the photolysis of $[(NC)_5Co^{III}-NC-Os^{II}(CN)_5]^{6-}$ leads via photoinduced electron transfer to the reactants from which it was formed by a thermal reaction, namely $[Co^{II}(CN)_5]^{3-}$ and $[Os^{III}(CN)_6]^{3-}$.[4c] However, to the best of our knowledge, the observation of a photoinduced two-electron charge-transfer based on a MMCT transition, as observed in the current case, has not previously been observed.

Conclusions

Since all of the photochemical experiments described were carried out at low light intensity (i.e. <75 mW/cm^2) the possibility of a multiphoton event leading to a simultaneous two-electron charge transfer can be ruled out. Further, the electrochemical data indicating that the two iron centers are noninteracting rule out the presence of a ground-state molecular orbital, delocalized over the entire trinuclear complex, from which a photoinduced two-electron charge transfer might occur. Therefore, the most likely mechanistic pathway leading to the observed two-electron charge-transfer chemistry involves an initial one-electron excitation from one of the two iron centers to generate an excited-state Pt(III) species followed by a thermal charge transfer to form the observed products as follows:

$$[Fe(II)-Pt(IV)-Fe(II)]^{4-} + h\nu \rightleftharpoons [Fe(II)-Pt(III)]^{-} + [Fe(CN)_6]^{3-} \quad (3)$$

$$[Fe(II)-Pt(III)]^{-} \rightleftharpoons [Fe(CN)_6]^{3-} + [Pt(NH_3)_4]^{2+} \quad (4)$$

Acknowledgment. This work was supported by the National Science Foundation under Grant No. CHE-8700868. B.W.P. is grateful for a General Electric Fellowship covering part of the duration of this research.

Supplementary Material Available: Tables SI-SV, listing additional crystal structure determination parameters, all nonequivalent bond distances and bond angles, atomic coordinates and isotropic thermal parameters, and anisotropic thermal parameters, and Figure S1, depicting the unit cell under the conditions listed in the Experimental Section (7 pages); Table SVI, listing observed and calculated structure factors (17 pages). Ordering information is given on any current masthead page.

Contribution from the Department of Inorganic Chemistry, Royal Institute of Technology, S-10044 Stockholm, Sweden

Inner- and Outer-Sphere Complex Formation in Aqueous Erbium Halide and Perchlorate Solutions. An X-ray Diffraction Study Using Isostructural Substitution

Georg Johansson* and Haruhiko Yokoyama†

Received August 18, 1989

Intensity difference functions obtained from large angle X-ray diffraction measurements on isostructural erbium and yttrium halide and perchlorate solutions have been used to derive the coordination around the erbium ion in solutions of different concentrations and anion-metal ratios. Two well-defined coordination spheres can be distinguished in the radial distribution functions. In the first sphere the erbium ion coordinates 8.0 ± 0.3 H_2O molecules at a distance of 2.35 ± 0.01 Å. Halide ions and possibly perchlorate ions penetrate into this sphere only when present in very large concentrations. In the inner-sphere complexes then formed, the Er-Cl and the Er-Br bonding distances are found to be 2.7 ± 0.1 and 2.87 ± 0.02 Å, respectively. The halide ions are concentrated to the second coordination sphere, in which the ratio between the numbers of halide ions and water molecules is larger than the stoichiometric ratio. In these solvent-separated ion pairs (outer-sphere complexes), the Er-Cl and Er-Br distances are found to be 5.0 Å.

Introduction

The structures of the solvated lanthanide ions and their complexes in solution have been the subject of a large number of investigations. Most methods, however, are capable of giving only indirect evidence on the nature of the bonding between the metal ions and their ligands. Direct structural information can be obtained with the use of diffraction methods, which give radial distribution functions (RDF), from which the structures of the solvated ions and their complexes can be derived. The information on the structures, contained in the RDFs, is usually, however, obscured by other structural features of the solution, which can prevent an unambiguous determination of the structure around the metal ion. In an aqueous solution, for example, water-water distances often appear in the same region as metal-water and metal-ligand distances, and the contributions of the different types of interactions to the scattering data cannot easily be resolved.

By the use of scattering measurements from two isostructural solutions, containing metal ions with different scattering powers, the non-metal interactions, which are the same in the two solutions, can be eliminated and the part of the RDF involving the metal ions can be separated.[1,2] The coordination can then be studied independently of the remaining structure. For the lanthanides, yttrium can be used for this purpose. The three-valent lanthanide ions and the yttrium ion all have the same outer electron configuration and differ only in the number of 4f electrons. They interact mainly electrostatically with their surroundings, and the f electrons contribute little to the bonding. The chemical differences result primarily from the slight decrease in ionic radius with increasing atomic number. In its chemical characteristics, yttrium usually appears among the heavy lanthanoids close to Ho^{3+} and Er^{3+}. Their thermodynamic characteristics do not usually differ significantly, their ionic radii are nearly the same, and their crystal structures are isomorphous and usually show no significant differences between observed bond lengths. X-ray diffraction measurements on solutions of these ions support the assumption that they are isostructural.[3,4] In the present work, the Y-Er pair

† Present address: Department of Chemistry, Yokohama City University, Seto, Kanazawa-ku, Yokohama 236, Japan.

(1) Bol, W.; Gerritis, G. J. H.; vanEck, C. L. v. P. *J. Appl. Crystallogr.* **1970**, *3*, 486.
(2) Soper, A. K.; Neilson, G. W.; Enderby, J. E.; Howe, R. A. *J. Phys. C* **1977**, *10*, 1793.
(3) Johansson, G.; Wakita, H. *Inorg. Chem.* **1985**, *24*, 3047.

0020-1669/90/1329-2460$02.50/0

has been used to study the coordination around the metal ions in halide and perchlorate solutions. In solution these three-valent metal ions have well-defined first as well as second coordination spheres, and the method used offers a possibility of determining the distribution and the bonding of water molecules and anions in the different spheres as a function of concentration and anion–metal ratio.

In previous investigations no evidence for inner-sphere complex formation of lanthanide ions (Ln^{3+}) with perchlorate ions in aqueous solutions seems to have been found.[5] In chloride solutions, stability constants, β_1, for the formation of the first complex, $LnCl^{2+}$, are usually determined to be around 1.[6,7] The second complex, $LnCl_2^+$, is found only in the presence of a large excess of chloride and reliable values for β_2 seem to be difficult to obtain.[8] For the bromide complexes, the β_1 values are smaller than those for the chloride complexes,[8] and iodide forms only very weak complexes in aqueous solution.[6,7]

On the basis of thermodynamic[9] and spectroscopic[10] evidence and from ultrasonic absorption experiments,[11] it has been concluded that the chloro complexes are solvent separated; that is, they are outer-sphere complexes. Luminescence excitation spectroscopy of the $^7F_0 \rightarrow {}^5D_0$ transition of Eu(III), however, has given evidence for the formation of inner-sphere chloro complexes.[12] Also, isomer shifts obtained from ^{151}Eu Mössbauer spectra[13] have been interpreted to indicate that chloride ions enter the inner coordination sphere.

In an early X-ray investigation of aqueous solutions of $ErCl_3$ and ErI_3, Brady[14] concluded that Er^{3+} is octahedrally coordinated by H_2O molecules at a distance of 2.3 Å. The actually observed coordination number was slightly larger, however, ≈6.5. The shortest Er–Cl and Er–I distances were found to be 4.6 and 5.4 Å, respectively, indicating the presence of solvent separated ion pairs. Wertz and co-workers determined the coordination numbers to be 8.0 in aqueous $LaCl_3$,[15] $GdCl_3$,[16] and $NdCl_3$[17] solutions and found evidence for inner-sphere complexes of Gd^{3+} and Nd^{3+} in solutions in which 10 M hydrochloric acid was the solvent. Habenschuss and Spedding[18] concluded from X-ray diffraction measurements on very concentrated chloride solutions of all of the lanthanides that the coordination number changed from 9.0 in the beginning of the series to 8.0 for the heavier lanthanides. Their analysis of the electronic radial distribution functions, $D(r)$, was limited to the first coordination sphere, and H_2O–H_2O and Cl–H_2O interactions overlapping the metal–water interactions were approximated by Gaussian peaks. They found no evidence for inner-sphere complex formation with the chloride ion. From a neutron diffraction investigation of a concentrated $NdCl_3$ solution in D_2O using isotopic substitution, Narten and Hahn[19,20] determined the number of water molecules in contact with Nd^{3+} to be 8.5 ± 0.2 and could also determine the tilt angle of the bonded water molecules, that is the angle between the Nd–O bond and the line bisecting the two O–D bonds, to be 24 ± 4°.[21] In a similar investigation of a concentrated $DyCl_3$ solution, they found 7.4 ± 0.5 water molecules bonded to Dy^{3+} with a tilt angle of 17 ± 3°.[21]

Table I. Compositions of Solutions

soln	concn/mol·dm^{-3} [ErX_3]	concn/mol·dm^{-3} [YX_3]	unit vol (V)/Å^3	no. in a unit vol M^{3+}	X^-	H^+	Li^+	H_2O
ClO_4A	0.994		1671	1	3.270	0.270		49.2
		0.994	1671	1	3.272	0.272		49.2
ClO_4B	0.970		1712	1	9.54	6.54		34.2
		0.970	1712	1	9.54	6.54		34.5
ClO_4C	2.88		577	1	3.21	0.21		12.2
		2.88	577	1	3.21	0.21		12.2
ClA	1.000		1661	1	3.197	0.198		53.9
		1.000	1661	1	3.197	0.197		53.8
ClB	0.844		1968	1	10.26	0.17	7.10	55.3
		0.838	1982	1	10.26	0.13	7.14	55.9
ClC	2.407		690	1	3.058	0.058		21.5
		2.406	690	1	3.076	0.076		21.3
BrA	1.000		1661	1	3.174	0.174		52.9
		1.000	1661	1	3.174	0.174		52.8
BrB	0.840		1977	1	10.37	0.207	7.16	52.4
		0.840	1977	1	10.37	0.207	7.16	52.3

Experimental Section

Solutions were prepared by dissolving the oxides (Johnson Matthey 99.9%) in HCl, HBr, or $HClO_4$. A slight excess of acid (≈0.2 M in H^+) was maintained in order to avoid hydrolysis. Pairs of erbium and yttrium solutions were matched to have the same compositions.

Erbium and yttrium were analyzed by titration with EDTA at pH 5.0 with xylenol orange as indicator. The concentration of anion was determined for the chloride and the perchlorate solutions by passing a portion of the solution through a column with a cation exchanger and titrating the eluate with a standardized NaOH solution. The concentrations of bromide and also of chloride in the 1 M solution were determined both by titration using the Mohr method and by a gravimetric method with silver nitrate. The compositions of the solutions are given in Table I.

The X-ray diffraction measurements were made in a Rigaku θ-θ diffractometer using Ag Kα radiation (λ = 0.5608 Å) and a focusing LiF single-crystal monochromator. Mo Kα radiation was avoided since its wavelength (λ = 0.7107 Å) is close to the K absorption edge of yttrium, which results in fluorescence radiation. Measurements were taken at discrete points at intervals in θ of 0.1° ($0 < \theta < 25°$) or 0.25° ($25° < \theta < 70°$). About 100 000 counts were collected for each point, and each solution was scanned twice, which corresponds to a statistical error of about 0.2%. Exit slits of $^1/_6$, $^1/_2$, 1, and 2° were used to cover the whole θ range. After corrections for background radiation and for absorption, data for the different ranges were scaled to a common data set, which was used as input for the computer program for the analysis of the data.

Data Treatment

The data were treated by a version of the KURVLR program[22] modified for use on an IBM PC. After corrections for polarization in the sample and in the monochromator and for incoherent radiation not removed by the monochromator, the observed intensities, $I(s)$, where $s = 4\pi(\sin\theta)/\lambda$, were normalized to a stoichiometric unit of volume, V, corresponding to one metal ion. Scattering factors, $f(s)$, for the neutral atoms were taken from ref 23 and were corrected for the real part of the anomalous dispersion. Values for incoherent scattering were taken from Cromer and Mann[24] and were corrected for the Breit–Dirac effect.[23] The normalization factor, K, was calculated by comparing observed data in the high-angle part of the intensity curve with $\sum n_i\{f_i^2(s) + (\Delta f_i'')^2\}$, the independent coherent scattering calculated for the chosen stoichiometric unit of volume. A reduced intensity function, $i(s)$, was then calculated according to the expression

$$i(s) = K(I(s)) - \sum n_i\{f_i^2(s) + (\Delta f_i'')^2\}$$

where n_i is the number of atoms "i" in the stoichiometric volume.

(4) Johansson, G. *Pure Appl. Chem.* **1988**, *60*, 1773.
(5) *Gmelins Handbuch der Anorganischen Chemie*; Springer Verlag: Berlin, 1977; Vol. C5, p 89.
(6) *Gmelins Handbuch der Anorganischen Chemie*; Springer Verlag: Berlin, 1986; Vol. D4, pp 311, 322, 325.
(7) Sillen, L. G.; Martell, A. E. *Stability Constants*; The Chemical Society: London: 1964, Spec. Publ. No. 17, Supplement No. 1; 1971, Spec. Publ. No. 25.
(8) Fukusawa, T.; Kawasuji, I.; Mitsugashira, T.; Sato, A.; Suzuki, S. *Bull. Chem. Soc. Jpn.* **1982**, *55*, 726.
(9) Marcus, Y. *J. Inorg. Nucl. Chem.* **1966**, *28*, 209.
(10) Choppin, G. R.; Unrein, P. J. *J. Inorg. Nucl. Chem.* **1963**, *25*, 387.
(11) Reidler, J.; Silber, H. B. *J. Phys. Chem.* **1974**, *78*, 424.
(12) Breen, P. J.; Horrocks, W. D., Jr. *Inorg. Chem.* **1983**, *22*, 536.
(13) Greenwood, N. N.; Turner, G. E. *Inorg. Nucl. Chem. Lett.* **1971**, *7*, 389.
(14) Brady, G. W. *J. Chem. Phys.* **1960**, *33*, 1079.
(15) Smith, L. S.; Wertz, D. L. *J. Am. Chem. Soc.* **1975**, *97*, 2365.
(16) Steele, M. L.; Wertz, D. L. *J. Am. Chem. Soc.* **1976**, *98*, 4424.
(17) Steele, M. L.; Wertz, D. L. *Inorg. Chem.* **1977**, *16*, 1225.
(18) Habenschuss, A.; Spedding, F. H. *J. Chem. Phys.* **1979**, *70*, 2797; **1979**, *70*, 3758; **1980**, *73*, 442.
(19) Narten, A. H.; Hahn, R. L. *Science* **1982**, *217*, 1249.
(20) Narten, A. H.; Hahn, R. L. *J. Phys. Chem.* **1983**, *87*, 3193.
(21) Annis, B. K.; Hahn, R. L.; Narten, A. H. *J. Chem. Phys.* **1985**, *82*, 2086.
(22) Johansson, G.; Sandström, M. *Chem. Scr.* **1973**, *4*, 195.
(23) *International Tables for X-ray Crystallography*; Kynoch Press: Birmingham, England: 1968, Vol. 3; 1974, Vol. 4.
(24) Cromer, D. T.; Mann, J. B. *J. Chem. Phys.* **1967**, *47*, 1892. Cromer, D. T. *J. Chem. Phys.* **1969**, *50*, 4857.

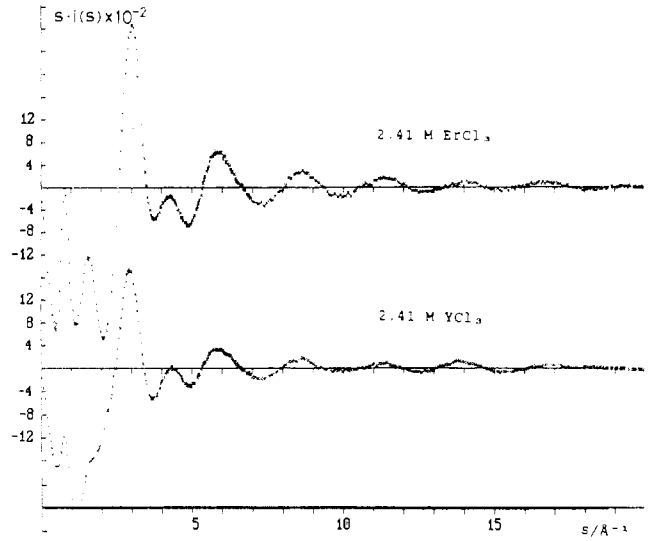

Figure 1. Comparison between observed $s(i(s))$ values for 2.41 M $ErCl_3$ and 2.41 M YCl_3 solutions.

Electronic radial distribution functions, $D(r)$, were obtained by a Fourier transformation

$$D(r) = 4\pi r^2\rho_0 + 2r\pi^{-1}\int_0^{s_{max}} s(i(s))(M(s))(\sin(rs))\,ds$$

$M(s)$ is a modification function chosen to be $(f_0^2(0))(f_0^{-2}(s)) \times (\exp(-0.01s^2))$ and $\rho_0 = (\sum n_i Z_i)^2/V$ with Z_i the atomic number for the atomic species "i".

Spurious peaks below 1.0 Å in $D(r)$, not attributable to interatomic distances, were used to correct the reduced intensities for low-frequency additions.[22]

For one of the pairs, the 2.4 M $ErCl_3$ and YCl_3 solutions, the reduced intensities, $s(i(s))$, are shown in Figure 1. The corresponding RDFs, $D(r)$, and the reduced RDFs, $D(r) - 4\pi r^2\rho_0$, are compared in Figure 2.

Separation of Interactions

The number of different pair interactions in a solution containing n atomic species is $n(n+1)/2$. For each pair interaction a partial structure function, $S_{pq}(s)$, can be defined and the total structure function for the solution can be written as the sum over the different partial structure functions. The reduced intensity observed in an X-ray diffraction experiment correponds to a sum over the different partial structure functions, each weighted by the product of the scattering factors for the two atomic species involved. For an aqueous solution, containing n_M metal ions, M, and n_X halide ions, X, in the stoichiometric unit the reduced intensity function can then be written

$$i(s) = 2n_Mn_X(f_M(s))(f_X(s))\{S_{MX}(s) - 1\} + 2n_Mn_0(f_M(s)) \times (f_0(s))\{S_{M0}(s) - 1\} + 2n_Mn_H(f_M(s))(f_H(s))\{S_{MH}(s) - 1\} + n_M^2(f_M^2(s))\{S_{MM}(s) - 1\} + 2n_Xn_0(f_X(s))(f_0(s))\{S_{X0}(s) - 1\} + 2n_Xn_H(f_X(s))(f_H(s))\{S_{XH}(s) - 1\} + n_X^2(f_X^2(s))\{S_{XX}(s) - 1\} + 2n_0n_H(f_0(s))(f_H(s))\{S_{0H}(s) - 1\} + n_0^2(f_0^2(s))\{S_{00}(s) - 1\} + n_H^2(f_H^2(s))\{S_{HH}(s) - 1\}$$

For two metal ions, M and M′, forming isostructural solutions, interactions that do not involve the metal ions are identical and are eliminated in the difference function

$$\Delta i(s) = i_M(s) - i_{M'}(s) = 2n_Mn_X(\Delta f_M(s))(f_X(s))\{S_{MX}(s) - 1\} + 2n_Mn_0(\Delta f_M(s))(f_0(s))\{S_{M0}(s) - 1\} + 2n_Mn_H(\Delta f_M(s))(f_H(s))\{S_{MH}(s) - 1\} + n_M^2[f_M^2(s) - f_{M'}^2(s)]\{S_{MM'}(s) - 1\}$$

where $\Delta f_M(s) = f_M(s) - f_{M'}(s)$.

The first two terms will be dominant in this expression. Because of the low scattering power of H for X-rays, the third term will be much smaller, although it cannot always be neglected. The fourth term will be neglected in the following since the distances of interest in this context will be small ($\lesssim$6 Å) and no polynuclear complexes are assumed to occur in the solutions studied.

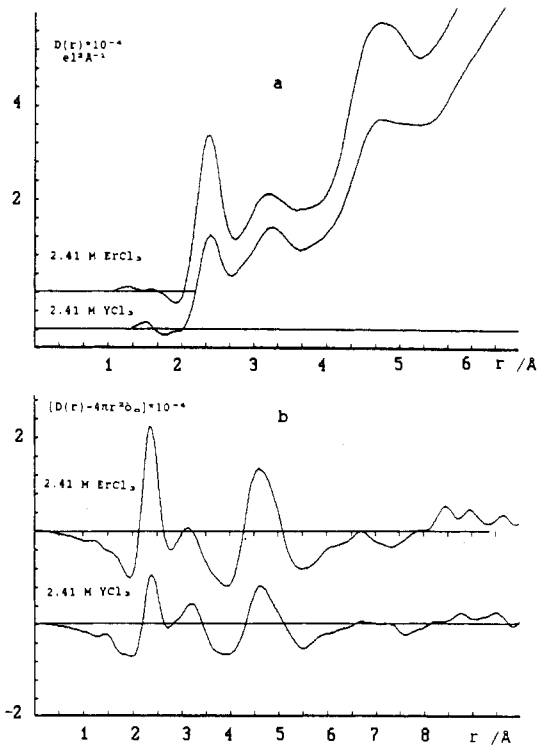

Figure 2. Comparison between the $D(r)$ functions (a) and the $D(r) - 4\pi r^2\rho_0$ functions (b) for 2.41 M $ErCl_3$ and 2.41 M YCl_3 solutions.

By using the convolution function $f_{Er}(s)/[f_{Er}(s) - f_Y(s)]$ a Fourier transformation of $\Delta i(s)$ gives the part of the RDF involving the erbium ion, which is the sum over the different partial RDFs

$$D^{Er}(s) = 4\pi r^2\rho_0^{Er} + 2r\pi^{-1}\int_0^{s_{max}} s(\Delta i(s))(\sin(rs))(M(s)) \times (f_{Er}(s))[f_{Er}(s) - f_Y(s)]^{-1}\,ds$$

where $\rho_0^{Er} = (\sum n_i Z_i)^2/V$ includes terms involving the erbium ion only.

The difference functions, $s(\Delta i(s))$, for the eight pairs of solutions investigated are shown in Figure 3. For the Fourier transformation the experimental $s(\Delta i(s))$ values were used directly without applying any smoothing function. The resulting $D^{Er}(r)$ functions are shown in Figure 4. For the 1 M solutions, the reduced RDFs and their separation into metal and non-metal interactions are shown in Figure 5.

Theoretical Peaks

Peaks in the derived $D(r)$ functions can be analyzed by comparison with theoretical peaks. For a specific type of interaction between two atoms p and q with a bonding distance equal to r_{pq}, the contribution to the reduced intensity is, according to the Debye expression, assuming a Gaussian distribution of the distances

$$i_{pq}(s) = a_{pq}n_pn_q(f_p(s))(f_q(s))(\sin(rs))(rs)^{-1}\exp(-\tfrac{1}{2}l_{pq}^2s^2)$$

where $a_{pq} = 1$ if $p = q$ and $a_{pq} = 2$ if $p \neq q$, n_p and n_q are the number of involved atoms p and q in the stoichiometric unit and l_{pq} is the root mean square variation in the distance r_{pq}. A Fourier inversion gives the corresponding contribution, p_{pq}, to the RDF:

$$p_{pq}(r) = 2r\pi^{-1}\int s(i_{pq}(s))(\sin(rs))(M(s))\,ds$$

By comparison of observed and calculated peaks, the parameters describing a particular type of interaction can be determined, that is the distance, r_{pq}, the frequency, n_{pq}, and the rms variation, l_{pq}.

The derivation of the $D^{Er}(r)$ function is based on the assumption that the Er^{3+} and the Y^{3+} ionic radii are equal. A slight difference in bond length will introduce an error that will primarily result in a small shift in the peak positions. The experimental data show the differences in Er^{3+} and Y^{3+} bonding distances to be small ($\lesssim$0.01 Å) and it will be ignored in the following. An alternative method, not used here, of analyzing the data, which would take

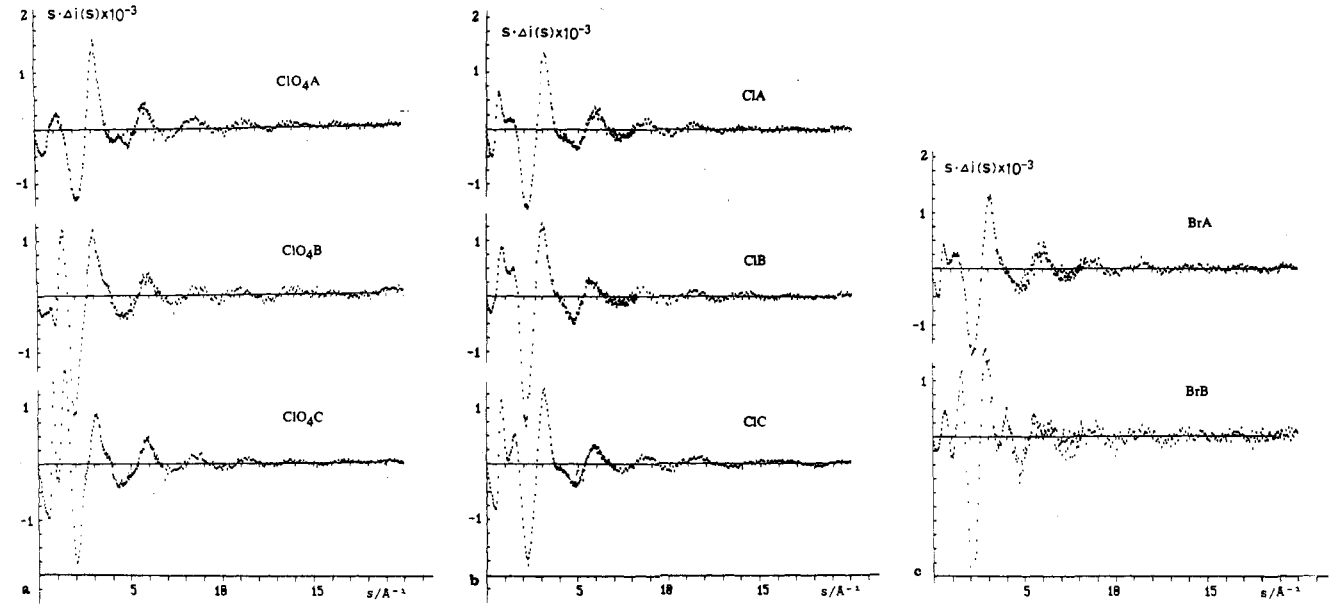

Figure 3. Intensity difference functions, $s(\Delta i(s)$, for the solutions investigated: (a) perchlorate solutions; (b) chloride solutions; (c) bromide solutions.

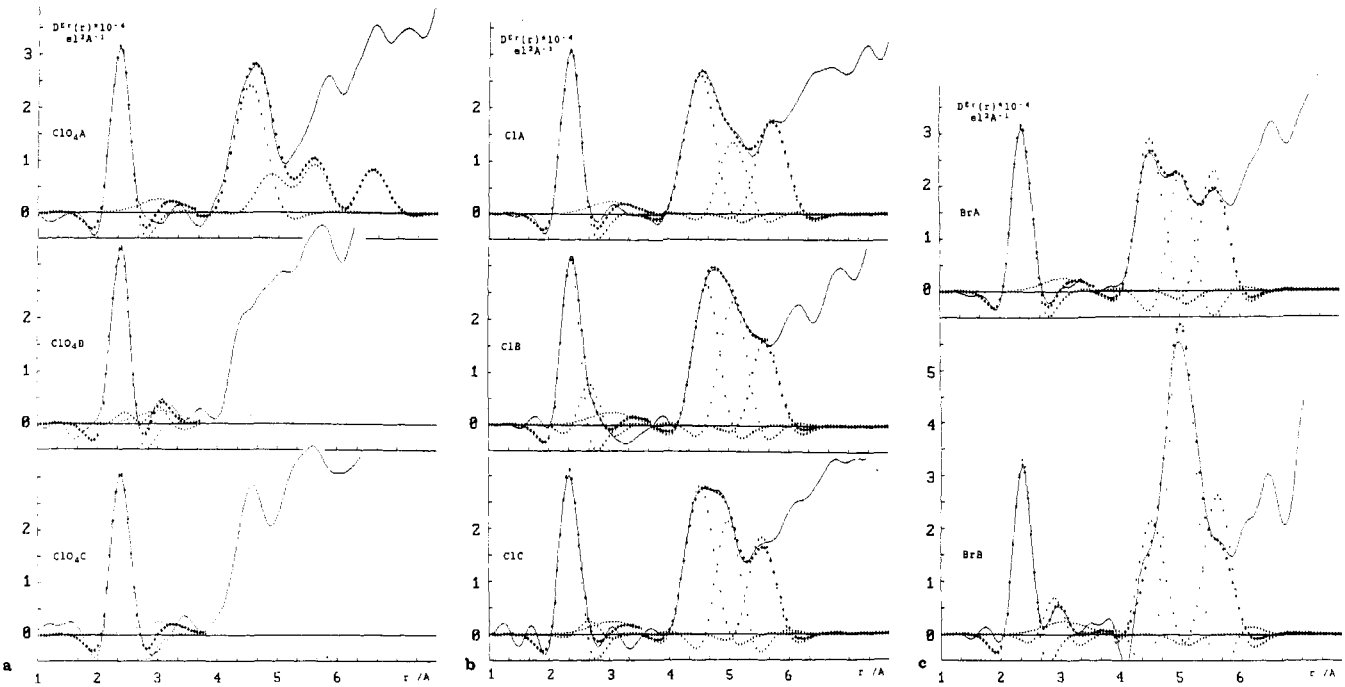

Figure 4. RDFs, $D^{Er}(r)$, calculated from the intensity difference functions (solid lines): (a) perchlorate solutions; (b) chloride solutions; (c) bromide solutions. Theoretical values, calculated as the sum over the individual interactions by using parameter values given in Table II for the first and in Table III for the second coordination sphere, are indicated by filled squares. The individual interactions are marked by crosses. For the halide solutions a second Er–H_2O peak, not listed in Table III, is included with the parameter values; r = 5.6 (1) Å, n = 9 (1), and l = 0.20 (5) Å. Contributions from hydrogen atoms to the second coordination sphere have been approximated by including Er–H interactions with r = 5.0 Å and l = 0.35 Å.

such a difference into account, is to use the Fourier transformation of the difference function, $\Delta i(s)$, without deconvoluting and compare the resulting peaks with theoretical peaks obtained as the difference between Er–X and Y–X interactions.[3]

Analysis of the Data

The scattering data for each solution have been normalized to a stoichiometric unit of volume containing one metal ion. The $D^{Er}(r)$ functions in Figure 4 are, therefore, all referred to one erbium ion and can be directly compared. Two well-defined coordination spheres are clearly indicated. The first peak at 2.35 Å is fully resolved from the peak at about 4.5 Å, corresponding to the second sphere, which is, however, partially overlapped by longer interactions. Beyond the peak of the second coordination sphere there are no pronounced peaks in the RDFs and therefore no marked ordering around the Er^{3+} ion (Figure 5).

For the non-metal interactions, the reduced radial distribution functions, which are given in Figure 5 for the 1 M solutions, show peaks expected for contact distances H_2O–H_2O (≈2.8 Å), Cl–H_2O (≈3.23 Å), Br–H_2O (≈3.35 Å), and Cl–O and O–O in ClO_4 (1.45 and 2.4 Å). A comparison between the separated (b and c) and the non-separated (a) RDFs in Figure 5 shows the overlap of peaks involving the Er^{3+} ion with those of the non-metal interactions, which will prevent a quantitative analysis of the coordination around Er^{3+} unless a separation of interactions can be made.

The First Coordination Sphere. Results of an analysis of the first coordination sphere by comparison of the observed peaks with theoretical peaks are shown in Figure 4 and Table II.

For the 1 M solutions without an excess of anion (ClO_4A, ClA, and BrA), the experimental peaks are apparently identical and can be closely reproduced by single Gaussian peaks. Parameter values corresponding to the best fit are given in Table II, and the

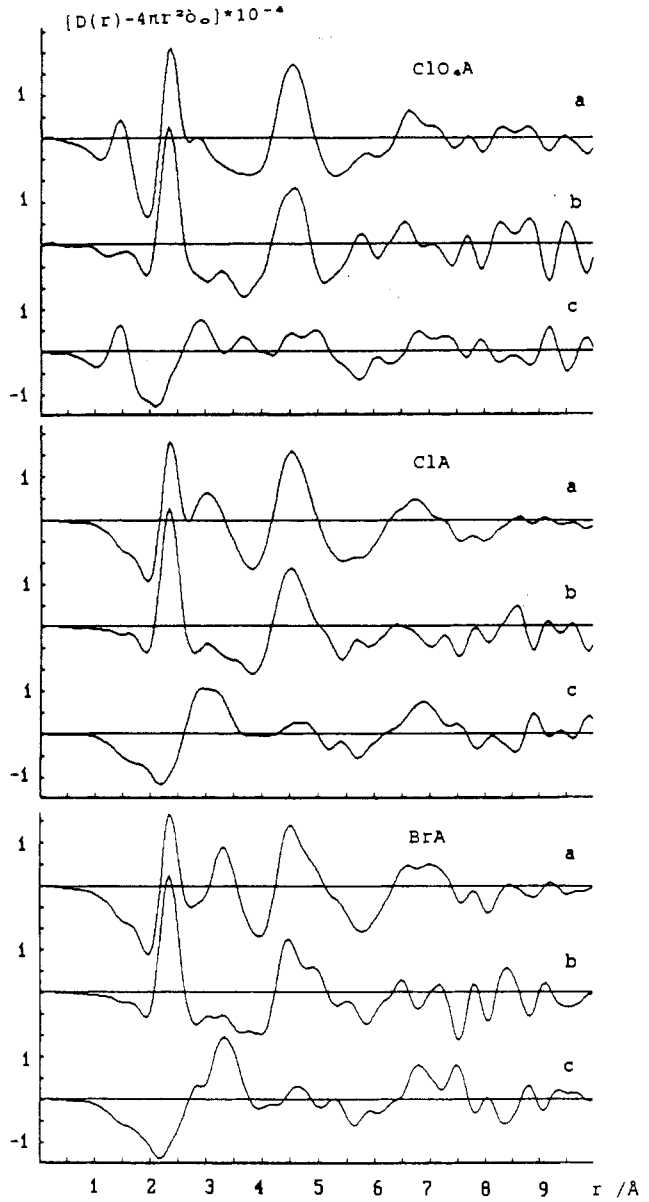

Figure 5. Reduced radial distribution functions for the 1 M solutions. For each solution, the nonseparated RDF (curves "a"), the part involving the Er interactions (curves "b"), and the part involving only non-erbium interactions (curves "c") are shown.

Table II. Derived Parameter Values for the First Coordination Sphere

	Er–O(H_2O)			Er–X		
soln	r/Å	n	l/Å	r/Å	n	l/Å
ClO_4A	2.35 (1)	8.0 (3)	0.089 (12)			
ClO_4B[a]	2.360 (15)	8.0 (3)	0.089 (9)	3.00 (8)[b]	0.31 (8)	0.08 (4)
ClO_4C	2.365 (15)	7.9 (3)	0.093 (11)			
ClA	2.35 (1)	8.0 (3)	0.095 (8)			
ClB	2.35 (1)	7.8 (8)	0.077 (13)	2.67 (7)	0.8 (3)	0.11 (5)
ClC	2.333 (15)	7.8 (3)	0.084 (12)	2.65 (10)	0.25 (15)	0.10 (4)
BrA	2.35 (1)	8.1 (3)	0.095 (8)			
BrB	2.35 (1)	7.9 (3)	0.07 (1)	2.87 (2)	0.3 (1)	0.11 (2)

[a] If no inner-sphere complex formation with ClO_4^- is assumed, a satisfactory fit can still be obtained by using the following parameter values for Er–O: r = 2.360 (15) Å, n = 8.5 (5), and l = 0.089 (12) Å. [b] The Er–Cl distance for a bidentate ClO_4^- ion.

agreement between observed and calculated peaks is shown in Figure 4. The estimated errors, which are given within brackets in Table II, are maximum errors indicating deviations, which lead to clear differences between observed and calculated peaks. In view of the estimated errors there are no significant differences between the parameter values obtained for the different solutions: the distance r = 2.35 ± 0.01 Å, the coordination number n = 8.0 ± 0.3, and the rms variation in the distance l = 0.09 ± 0.01 Å. The results demonstrate that in these solutions only water molecules are included in the coordination sphere and inner-sphere complexes are not formed. It is also obvious that a coordination with nonequivalent water molecules, which is found in some crystal structures,[25] does not occur in solution.

Table III. Derived Parameter Values for the Second Coordination Sphere

	Er–O(H_2O)			Er–X		
soln	r/Å	n	l/Å	r/Å	n	l/Å
ClO_4A	4.50 (5)	13 (1)	0.26 (4)	5.6 (2)[a]	2 (1)	0.24 (4)
ClA	4.51 (4)	13.2 (15)	0.24 (4)	5.07 (8)	2.8 (7)	0.24 (4)
ClB	4.60 (4)	11.0 (10)	0.20 (5)	5.06 (6)	4.8 (5)	0.24 (4)
ClC	4.50 (2)	12.8 (10)	0.22 (4)	4.98 (2)	3.5 (4)	0.20 (3)
BrA	4.49 (1)	12.0 (8)	0.20 (3)	5.01 (1)	1.6 (2)	0.20 (3)
BrB	4.5 (1)	9 (1)	0.2 (1)	5.00 (2)	5.2 (5)	0.25 (3)

[a] Er–Cl(ClO_4^-) distance.

Neutron diffraction investigations on concentrated $NdCl_3$[19,20] and $DyCl_3$[21] solutions have shown the water molecules in the first coordination sphere to have a preferred orientation, which leads to well-defined metal–hydrogen distances. Although the contributions from corresponding Er–H distances to the X-ray scattering are small, because of the low scattering power of hydrogen for X-rays, they are not negligible and they have been included in the analysis of the first coordination sphere. Their contributions, using the parameter values r_{Er-H} = 3.0 Å, l_{Er-H} = 0.24 Å, and n_{Er-H} = 16.0, are separately drawn in Figure 4.

An increase in the anion concentration by addition of LiCl or LiBr to the halide solutions and of $HClO_4$ to the perchlorate solution leads to slight changes in the first coordination peaks (ClO_4B, ClB, and BrB in Figure 4). These changes can be related to a penetration of anions into the first coordination sphere. In the chloride solution (ClB), the peak is slightly broadened toward longer distances. In the bromide solution (BrB), the 2.35-Å peak is unchanged, but a new peak appears at about 2.9 Å. In the perchlorate solution (ClO_4B), the 2.35-Å peak is slightly changed and a minor peak appears at about 3.0 Å. These are expected changes if inner-sphere complexes are formed. Er–Cl bond lengths in crystal structures are found to be about 2.7 Å, which is too close to the 2.35 Å Er–O distance to lead to a separate peak in the RDFs, but it results in a broadening of the peak. The larger ionic radius of the bromide ion leads to an expected Er–Br distance of about 2.9 Å, which differs sufficiently from the Er–O distance to lead to a separate peak. In the perchlorate solution a bidentate bonding of ClO_4^- to Er^{3+} with an Er–Cl distance of 3.0 Å is consistent with the observed changes (ClO_4B in Figure 4).

The observed peaks in the "B" solutions were analyzed on this basis and the results are given in Table II and in Figure 4. The analysis shows that the inner-sphere complex formation is weak with an average number of only about 0.8 Cl^- bonded to each Er^{3+} ion in the chloride solution. In the bromide solution, the complex formation is weaker and only about 0.3 Br^- ion is bonded. About the same number is found for the ClO_4^- ion in the perchlorate solution. The Er–H_2O distances and their rms variations do not differ significantly from the values found for the "A" solutions. In view of the estimated errors, no definite conclusions can be made about a possible change in the total coordination number when the complexes are formed.

In the concentrated perchlorate solution, ClO_4C, the first coordination peak can be described by the same parameter values as were used for the 1 M solution (Table II and Figure 4), and no inner-sphere complex formation is indicated. In the concentrated chloride solution, a slight broadening of the peak may be explained by an incorporation of about 0.2 Cl^- ion into the first coordination sphere (Table II and Figure 4).

The Second Coordination Sphere. Peaks corresponding to interactions between erbium and a second coordination sphere are

(25) Chatterjee, A.; Maslen, E. N.; Watson, K. J. *Acta Crystallogr.* **1988**, *B44*, 381.

Table IV. Relative Distribution of Ligands with the Numbers Given for the Ligands in the Different Coordination Spheres Referred to a Stoichiometric Unit of Volume Containing One Erbium Atom

	stoichiometric			first sphere			second sphere			bulk		
soln	H_2O	X^-	X^-/H_2O	H_2O	X^-	X^-/H_2O	H_2O	X^-	X^-/H_2O	H_2O	X^-	X^-/H_2O
ClO_4A	49.2	3.27	0.07	8.0	0.0	0.0	13.0	2.0	0.15	28.2	1.3	0.05
ClA	53.9	3.20	0.06	8.0	0.0	0.0	13.2	2.8	0.21	32.7	0.4	0.01
ClB	55.5	10.3	0.19	7.8	0.8	0.10	11.0	4.8	0.44	36.7	4.7	0.13
ClC	21.4	3.07	0.14	7.8	0.3	0.03	12.8	3.5	0.27	0.8	−0.7[a]	−0.9[a]
BrA	52.8	3.17	0.06	8.1	0.0	0.0	12.0	1.6	0.13	32.8	1.6	0.05
BrB	52.3	10.4	0.20	7.9	0.3	0.04	8.5	5.2	0.61	36.0	4.9	0.14

[a] Negative values indicate sharing of atoms between coordination spheres of different Er^{3+} ions.

present for all of the solutions investigated. Although these peaks are not completely separated from longer distances, they can be approximately analyzed in terms of Er–H_2O and Er–anion interactions.

In the 1 M solutions with no excess of anion, the second coordination peak appears at 4.5 Å. In the perchlorate and the chloride solutions, the peaks are similar but have some distinct differences, which indicate that anions are also involved here. In the bromide solution, the 4.5-Å peak is partly overlapped by a peak at 5.0 Å. On addition of anion, the 5-Å peak in the bromide solution increases and a similar change is observed for the chloride solution (Figure 4). In the perchlorate solution, the second coordination peak smears out on addition of $HClO_4$ and is no longer separated from longer interactions (Figure 4).

These observations indicate that the 4.5-Å peaks correspond to Er–H_2O distances and the 5-Å peaks to Er–Cl and Er–Br distances. An analysis of the second coordination peaks in terms of these interactions leads to the results in Table III and in Figure 4. A peak at 5.6 Å, which is present in the halide solutions, has been included in this analysis, assuming it to represent Er–H_2O interactions. For the 1 M perchlorate solution, which is the only perchlorate solution with a sufficiently well-separated second coordination peak to allow an analysis, a good fit is obtained by assuming about two perchlorate groups to be bonded to Er^{3+} in a bidentate way. In the chloride and the bromide solutions, the anions are found to be present in the second coordination sphere not only in the excess anion solutions, where the Er-halide interactions lead to separate peaks, but also in the absence of an excess of anion (Figure 4). The total coordination number for the second coordination sphere is found to be about twice that for the first sphere.

The experimental uncertainties, which can be seen as ripples in the $D(r)$ functions, the incomplete separation of the second coordination sphere peak from longer interactions, and the small difference in Er–H_2O and Er–halide distances, make this analysis less precise than that of the first coordination sphere, which is reflected in the larger estimated errors given in Table III.

Discussion

The combination of X-ray diffraction measurements from two isostructural solutions of the same compositions, one containing Er^{3+} and the other containing Y^{3+}, has made it possible to separate the interactions involving the metal ions from those of the nonmetal interactions. The resulting radial distribution functions (Figure 4 and 5), calculated from the intensity difference curves (Figure 3), give information on the surroundings of the Er^{3+} ion in the solution, which is not obscured by contributions from non-metal interactions. They show the presence of two well-defined coordination spheres around the Er^{3+} ion. Beyond the second coordination peak, however, the deviations from an average distribution are small. For each solution the peak in the RDF corresponding to the first coordination sphere is fully separated from that of the second coordination sphere, and it can be analyzed in detail by comparison with theoretical peaks.

For all perchlorate, chloride, and bromide solutions investigated, the Er^{3+} ion is found to have a coordination number of 8.0 ± 0.3 independent of concentration and of counterion. Chloride and bromide ions do not penetrate the first coordination sphere except when present at very high concentrations. The chloride ion has a stronger tendency than the bromide ion to form inner-sphere complexes. In the 1 M erbium halide solutions with X^-:Er^{3+} ratios of about 10 (Table I) an average of 0.8 Cl^- or 0.3 Br^- is found in the first coordination sphere (Table II). The corresponding distances are 2.67 Å for Er–Cl, 2.87 Å for Er–Br, and 2.35 Å for Er–H_2O (Table II).

The Er–Cl and the Er–O distances found for the innersphere complexes in the chloride solution do not differ significantly from those found in crystal structure determinations of the two isomorphous compounds $[ErCl_2(OH_2)_6]Cl$ and $[YCl_2(OH_2)_6]Cl$.[26] These crystals contain discrete $[MCl_2(OH_2)_6]^+$ cations with Er–Cl = 2.730 (3) Å and Y–Cl = 2.747 (1) Å and with Er–O = 2.36 (3) Å and Y–O = 2.35 (2) Å. (Figures given within brackets are standard deviations.) The Er–Br bond length of 2.87 Å found in the bromide solution is about 0.20 Å longer than that of Er–Cl, which is consistent with the difference between their ionic radii.

The second coordination sphere contains both water molecules and anions and is strongly dependent on concentration, type of anion, and the anion:metal ratio (Table III and Figure 4). In the 1 M solutions with no excess of anion, water is the dominant constituent and the number of H_2O molecules in the second coordination sphere corresponds approximately to the number of hydrogen bonds that can be formed by the eight H_2O molecules in the first coordination sphere.

The distances from the Er^{3+} ion to the units bonded in the second coordination sphere are found to be 4.50 Å for Er–H_2O and 5.0 Å for Er–Cl and for Er–Br. A comparison with corresponding distances in the crystal structures of $[ErCl_2(OH_2)_6]Cl$ and $[YCl_2(OH_2)_6]Cl$, shows that in the crystals Er–Cl distances are 4.99–5.21 Å (average 5.054 Å) and Y–Cl distances are 4.95–5.20 Å (average 5.044 Å) to six Cl^- ions, which are not bonded in another $ErCl_2(H_2O)_6$ unit. The distances to six other Cl^- ions, which belong to another such unit, are for Er–Cl 4.79–5.01 Å (average 4.875 Å) and for Y–Cl 4.77–4.99 Å (average 4.879 Å). In the crystal structures, all water molecules, which can be included in a second coordination sphere, belong to other $[MCl_2(OH_2)_6]^+$ units and are not directly comparable to those in the solutions. The shortest Er–H_2O distances involve four H_2O and are 4.917 Å in the Er compound and 4.918 Å in the Y compound.

Because of the low scattering power of the hydrogen atoms, their positions cannot be determined from the X-ray diffraction measurements and cannot be used for a determination of the orientation of the water molecules in the first coordination sphere. It seems likely, however, that the geometrical arrangement of water molecules in the second coordination sphere is determined by the formation of hydrogen bonds from water molecules in the first sphere, and by using reasonable assumptions about hydrogen bonding, it is possible to make an estimate of the orientation of the water molecules in the first coordination sphere. From the experimentally determined distances between the erbium ion and the water molecules in the first and second coordination spheres, assuming linear hydrogen bonds with O–H distances of 0.96 Å, the angle between the Er–H_2O bond and the line bisecting the two O–H bonds can be estimated to be about 30°. This value for the tilt angle of the water molecules is of the same order of magnitude as the value of about 20° found in neutron diffraction investigations of $NdCl_3$ and $DyCl_3$ solutions in which the hydrogen

(26) Rogers, R. D.; Kurihara, L. K. *Lanthanide Actinide Res.* **1986**, *1*, 295.

positions could be experimentally determined.[21]

Conclusions

The analysis of the diffraction data show conclusively that in aqueous erbium halide and perchlorate solutions the metal ion is coordinated by eight water molecules with an Er–H_2O distance of 2.35 Å. This is independent of concentration and of anion in the solutions investigated. Inner-sphere complexes are formed only at very high ligand concentration and then only to a small extent. The Er–Cl distances in these ion pairs do not differ significantly from corresponding distances in known crystal structures.[26]

The erbium ion also has a well-defined second coordination sphere containing both water molecules and anions, with Er–H_2O distances of about 4.50 Å. The Er–Cl and Er–Br distances in these solvent-separated ion pairs are about 5.0 Å and are not significantly different although the Br^- ionic radius is larger than that of Cl^-. This might be caused by the difference in the ability of Cl^- and of Br^- to form hydrogen bonds. In a preliminary investigation of an iodide solution the corresponding Er–I distance is found to be 5.25 Å. The increase corresponds to the difference in ionic radii between Br^- and I^-.

The number of halide ions and of water molecules in the two coordination spheres and in the remaining part of the solution, not involved in the coordination around erbium, can be estimated from the results given in Tables I–III. The values obtained are compared in Table IV with the stoichiometric compositions of the solutions and show that the water molecules are the preferred ligands in the first coordination sphere but the halide ions are concentrated in the second coordination sphere.

If the erbium halide solutions are described in terms of inner- and outer-sphere complexes, the diffraction measurements lead to the conclusion that inner-sphere complexes are formed only at very high ligand concentrations but outer-sphere complexes are extensively formed even at relatively low concentrations. The first coordination sphere of the erbium ion is occupied almost exclusively by water molecules. The halide ions are concentrated in the distinct second coordination sphere, where the halide:water ratio is larger than the stoichiometric ratio (Table IV).

Acknowledgment. Support from the Swedish Natural Science Research Council (NFR), from the foundation "Knut and Alice Wallenbergs Stiftelse", and from the Ministry of Education in Japan for H.Y. is gratefully acknowledged. We are indebted to E. Hansen and I. Desselberger for technical assistance.

Registry No. H_2O, 7732-18-5; $Er(ClO_4)_3$, 14017-55-1; $ErCl_3$, 10138-41-7; $ErBr_3$, 13536-73-7; Er, 7440-52-0; YCl_3, 10361-92-9.

Contribution from the Department of Chemistry and Materials Science Center, Cornell University, Ithaca, New York 14853-1301

Bonding in the Two-Dimensional Cu–Ga Layer of a Ca_2Cu_2Ga Crystal

Christian Kollmar and Roald Hoffmann*

Received September 7, 1989

We have examined the bonding properties of a two-dimensional layer containing linear Cu chains and unusual four-coordinate Ga atoms in a Ca_2Cu_2Ga crystal. The bond length between two Cu atoms bridged by two Ga atoms is slightly increased as compared to the bond length between two unbridged Cu atoms. We first calculated the band structure of a one-dimensional linear Cu chain and then introduced the Ga sublattice, thus forming the two-dimensional layer. The construction reveals how the bonding between the Ga-bridged Cu atoms vanishes almost completely, whereas the other Cu–Cu bond strength is not much affected. This is due to substantial mixing of Ga p orbitals into the symmetric intra-unit-cell linear combination of the Cu s orbitals in parts of the Brillouin zone, thus significantly weakening the Cu–Cu bond. For symmetry reasons, no such mixing is allowed for the antisymmetric linear combination of the Cu s orbitals. Introducing the Ca atoms to form the full three-dimensional structure has no major effect on Cu–Cu and Cu–Ga bonding but does place one partially filled Ca band in the valence region. Ca_2Cu_2Ga should be a conductor, unlikely to be subject to Peierls distortions. It should be possible to increase Cu–Ga bonding by feeding electrons into the Cu_2Ga sublattice.

Introduction

Recently, an investigation of the structure of some MCuGa compounds (M = Ca, Sr, Ba) has been published.[1] These compounds show unusual coordination geometries around Cu and Ga. For instance, one of them consists of linear Cu chains linked to two-dimensional layers through bridging Ga atoms. Linear metal chains are rare and so are the four-coordinate planar Ga atoms. The structure of this Ca_2Cu_2Ga compound is shown in **1**. The structural type is body centered orthorhombic, isotypic with Pr_2Ni_2Al.[2] **1** shows a three-dimensional view along the *a* axis of the crystal. The Ga atoms are represented by the hatched spheres, the Cu atoms by the smaller blank spheres, and the Ca atoms by the larger blank spheres. Since the distances between the Ca atoms and their nearest neighbors are larger than 3 Å, we neglect the corresponding Ca–Ga and Ca–Cu interactions in a first approach and treat the problem in two dimensions. The relevant two-dimensional slab of Cu_2Ga^{4-} is shown in **2**. It constitutes the *a*–*b* plane with the *b* axis oriented along the Cu chains.

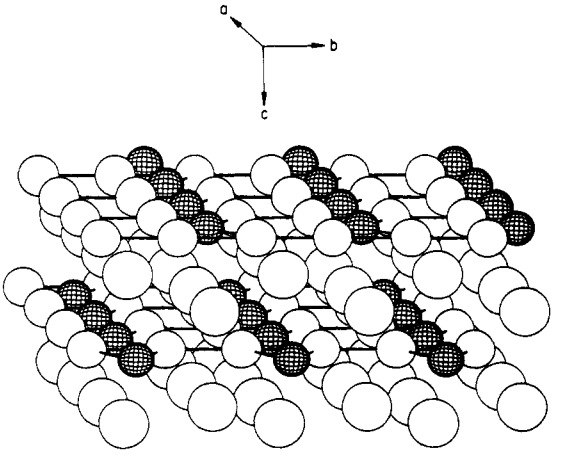

1

Note the linear Cu chains, nearly equally spaced at distances of 2.70 and 2.78 Å. The separations are longer than in Cu metal

(1) Fornasini, M. L.; Merlo, F. *J. Less-Common Met.* **1988**, *142*, 289.
(2) Rykhal, R. M.; Zarechnyuk, O. S.; Kuten, Ya. I. *Dopov. Akad. Nauk Ukr. RSR, Ser. A* **1978**, 1136.

0020-1669/90/1329-2466$02.50/0